




Stable, Spherical and Thin Fluid Shells

George Alestas ^{1,t} , George V. Kraniotis ^{2,t}  and Leandros Perivolaropoulos ^{3,t} ¹ g.alestas@uoi.gr² gkraniotis@uoi.gr³ leandros@uoi.gr[†] Current address: Department of Physics, University of Ioannina, 45110 Ioannina, Greece

Abstract: We consider and prove the existence of stable, spherical, and thin fluid shells in the context of a Schwarzschild-Rindler-anti-de Sitter (SRAdS) background. We identify the metric parameter regions that allow the existence and stability of these shells for three cases of fluid equations of state. The case of the vacuum shell is especially interesting since it remains consistent with past studies of two of the authors of this manuscript that showed the existence of stable spherical domain walls in the context of the same metric. This type of structures could be an alternative to the idea of the gravastar star formations.

Keywords: stability; fluid equation of state; gravastar; Rindler; anti- de Sitter; domain wall; spherical shell;

1. Introduction

The concept of a thin shell spherical shells in General Relativity holds great significance as a theoretical construct because as was first shown in [1], one can use it to model the interactions between matter and gravity and find analytical solutions to the Einstein equations governing them.

The gravastar [2–6] is such a theoretical, spherical, and stable thin shell configuration that can be used to accurately describe an alternative to black hole as the last step of stellar evolution. The concept of gravastars portray star structures that alternate between a Schwarzschild metric for its exterior and a de Sitter metric for its interior space, with the inner region considered traditionally as a gravitational Bose-Einstein condensate with zero entropy.

As shown in [7] a stable spherical thin shell solution similar to that of the gravastar can be found when considering a non-trivial background geometry of a Schwarzschild-anti-deSitter curved spacetime [7,8] with a Rindler acceleration term, coupled with spherically symmetric scalar field dynamical equations. This metric is a Schwarzschild-Rindler-anti-deSitter (SRAdS) metric [9],

$$ds^2 = f(r)dt^2 - \frac{dr^2}{f(r)} - r^2(d\theta^2 + \sin^2\theta d\phi^2) \quad (1)$$
$$f(r) = 1 - \frac{2Gm}{r} + 2br - \frac{\Lambda}{3}r^2$$

where Λ is the well known cosmological constant, and b is the parameter attributed to the Rindler acceleration .

This SRAdS metric (1) has been subject to constrains appended by solar system observations[10,11], it can produce flat rotation curves [12], and it has been shown to partially explain [13,14] the Pioneer anomaly [15,16].

A new analysis [17] was instigated by the fact that this type of metric has a demonstrated ability of supporting metastable structures such as spherical domain walls. Specifically the question that was raised was whether this metric could foster thin shell solutions



Citation: . *Proceedings* 2020, 0, 5.
<https://doi.org/>

Received:

Accepted:

Published:

Publisher's Note: MDPI stays neutral with regard to jurisdictional claims in published maps and institutional affiliations.



Copyright: © 2020 by the authors. Licensee MDPI, Basel, Switzerland. This article is an open access article distributed under the terms and conditions of the Creative Commons Attribution (CC BY) license (<https://creativecommons.org/licenses/by/4.0/>).

adhering to the three most general forms of equations of state, corresponding to a vacuum shell, a stiff matter shell and a dust shell.

In what follows we will show how we made use of the Israel junction conditions formalism to explore the aforementioned question by breaking it down to four simpler points of interest:

- Is it possible to construct stable, thin, fluid shells within a SRAdS metric?
- If so, which are the specific, general conditions that have to be met in order to achieve stability?
- What are the numerical metric parameter ranges that enable stability, considering the conditions induced by the different equations of state?
- How does the radius R of the stable shell change as a function of the metric parameters within the allowed numerical space?

As mentioned above we have made use of the Israel junction condition formalism in order to interpolate between the two metric parts of the shell, in each case of equations of state. The value of the shell mass m has been considered to be discontinuous radially across the shell, m_- inside and m_+ outside, in contrast to the values of the b and Λ parameters that are considered to have continuous fixed values when crossing the shell.

The manuscript is structured as follows: In the first section we show the general theory that has been developed entailing the derivation of stability conditions for a static and spherical shell with a general equation of state on a SRAdS metric background geometry. In section 3 we show how these results can be applied to three specific cases of fluid equations of state, as well as how we can derive the conditions for stability in each case. Finally, in the last section 4 of the manuscript, we discuss the opportunities for extending the analysis presented here.

The following assumptions have been made in the entirety of the manuscript: We set $G = c = 1$, as well as $m_- = 1$. For the parameter values considered here an event horizon exists but no cosmological horizon, and the shell radius is always outside the event horizon of the black hole.

2. Existence and Stability of Thin Shell Solutions

We begin by defining a spherical and thin shell with a radius R which alternates between an interior ($g_{\mu\nu}^-$) and an exterior ($g_{\mu\nu}^+$) SRAdS metric of the form [2,3,18],

$$ds^2 = f_{\pm}(r_{\pm})dt^2 - \frac{dr_{\pm}^2}{f_{\pm}(r_{\pm})} - r_{\pm}^2(d\theta^2 + \sin^2\theta d\phi^2) \quad (2)$$

where,

$$f_{\pm}(r_{\pm}) = 1 - \frac{2m_{\pm}(r_{\pm})}{r_{\pm}} \quad (3)$$

and

$$m_{\pm}(r_{\pm}) = m_{\pm} + \frac{\Lambda}{6}r_{\pm}^3 - br_{\pm}^2. \quad (4)$$

Considering the case of a shell in the context of the SRAdS metric (1) one can derive the Israel junction conditions in the form of [3]

$$p = \frac{1}{8\pi R} \left[\left[\frac{1 - m_{\pm}(R)' - m_{\pm}(R)/R + \dot{R}^2 + R\ddot{R}}{\sqrt{1 + \dot{R}^2 - 2m_{\pm}(R)/R}} \right] \right] \quad (5)$$

$$\sigma = -\frac{1}{4\pi R} \left[\left[\sqrt{1 + \dot{R}^2 - 2m_{\pm}(R)/R} \right] \right],, \quad (6)$$

where (') denotes the derivative of the mass with respect to r , and the dot corresponds to the derivative with respect to the proper time, defined as

$$d\tau^2 = - \frac{1}{1 - 2m_{\pm}(R)/R} \left[\frac{dR}{dt} \right]^2 + dt^2 \left[1 - \frac{2m_{\pm}(R)}{R} \right] dt^2. \quad (7)$$

From these equations one can derive the equation for the energy conservation of the shell

$$\frac{d}{d\tau}(\sigma R^2) + p \frac{d}{d\tau} R^2 = 0. \quad (8)$$

Then eq. (6) could be written as,

$$E = \frac{1}{2} \dot{R}^2 + V(R) \quad (9)$$

considering that,

$$V(R) \equiv 1 - \left[\frac{4\pi\sigma R^2}{2R} + \frac{m_+(R) + m_-(R)}{4\pi\sigma R^2} \right]^2 + \frac{4 m_+(R) m_-(R)}{16\pi^2\sigma^2 R^4} \quad (10)$$

and $E = 0$.

Therefore, the necessary general conditions for the existence and stability of a static fluid shell take the form,

$$\begin{aligned} V(R) &= 0 \\ V''(R) &> 0 \\ V'(R) &= 0, \end{aligned} \quad (11)$$

where we have made the assumption that eq. (9) is exactly the same as that of a particle moving in a straight line with zero energy. For the SRAdS metric the general form of the potential of the shell has the form

$$V(R) = 1 - \frac{\Lambda R^2}{3} - \frac{(m_- - m_+)^2}{16\pi^2 R^4 \sigma(R)^2} - \frac{m_- + m_+}{R} - 4\pi^2 \sigma(R)^2 R^2 + 2bR. \quad (12)$$

In what follows we show the derivation of the system of equations that constrain the ranges of (b, Λ) that permit the existence of stable, spherical fluid shells. Specifically, we concern ourselves with three distinct types of fluid shells, the vacuum, the stiff matter, and the dust fluid shell. We also derive the numerical ranges of the metric parameters that allow for stability.

3. Specific Cases of Shell Stability

3.1. Shell with vacuum fluid equation of state

Firstly, we concern ourselves with the case of the vacuum shell with an equation of state,

$$p = -\sigma. \quad (13)$$

Therefore the surface density takes the form,

$$\sigma(R) = \sigma_0 = \text{const.} \quad (14)$$

In this case the system of eqs. (11) necessary for the existence and stability of a shell solution becomes,

$$V(R) = 1 - \frac{m_- + m_+}{R} - \frac{\Lambda R^2}{3} - \frac{(m_- - m_+)^2}{16\pi^2 R^4 \sigma_0^2} - 4\pi^2 \sigma_0^2 R^2 + 2bR = 0, \quad (15)$$

$$\frac{\partial V}{\partial r} \Big|_{r=R} = 2b + \frac{m_- + m_+}{R^2} - \frac{2\Lambda R}{3} + \frac{(m_- - m_+)^2}{4\pi^2 R^5 \sigma_0^2} - 8\pi^2 \sigma_0^2 R = 0, \quad (16)$$

$$\frac{\partial^2 V}{\partial r^2} \Big|_{r=R} = -\frac{2\Lambda}{3} - \frac{2(m_- + m_+)}{R^3} - \frac{5(m_- - m_+)^2}{4\pi^2 R^6 \sigma_0^2} - 8\pi^2 \sigma_0^2 > 0. \quad (17)$$

Whereas its solution is written as

$$\Lambda(R, \sigma_0) = \frac{15(m_- - m_+)^2}{16\pi^2 R^6 \sigma_0^2} + \frac{6(m_- + m_+) - 3R}{R^3} - 12\pi^2 \sigma_0^2, \quad (18)$$

$$b(R, \sigma_0) = \frac{3(m_- - m_+)^2 + 8\pi^2 [3(m_- + m_+) - 2R] R^3 \sigma_0^2}{16\pi^2 \sigma_0^2 R^5}, \quad (19)$$

$$R > 3(m_- + m_+) \equiv R_{min} \quad (20)$$

$$\sigma_0 \equiv \frac{\sqrt{15} \sqrt{-\frac{(m_- - m_+)^2}{R^3(3m_- + 3m_+ - R)}}}{4\pi} + \Delta\sigma > \frac{\sqrt{15} \sqrt{-\frac{(m_- - m_+)^2}{R^3(3m_- + 3m_+ - R)}}}{4\pi} \equiv \sigma_{0min} \quad (21)$$

where $\Delta\sigma$ corresponds to perturbations of the surface density σ_0 .

The fact that the parameters R and σ_0 display lower limits as seen in eqs. (20), (21) allows us to derive boundaries on the values of (b, Λ) that permit the existence and stability of the stable shell solutions. These lower and upper boundaries are of the form,

$$\Lambda \rightarrow -\infty \implies b \rightarrow -\frac{1}{6(m_+ + m_-)} \quad (22)$$

$$\sigma_{0min} \rightarrow 0 \text{ and } \Lambda \rightarrow -12\pi^2 \sigma_0^2 > 0 \quad (23)$$

$$b < 0 \text{ with } \Lambda < \Lambda_{max} = -12\pi^2 \sigma_0^2. \quad (24)$$

In Fig. 1 [17] we can see the aforementioned boundaries as well as the parameter space that allows for stability considering the values of $m_+, m_- - m_+, m_-$. The minimum value of the parameter b is increased as m_+ is increased (see eq. (22)). For the three sets of (R, σ, b, Λ) displayed as color coded dots in the the right panel of Fig. 1 we show their corresponding potentials in Fig. 2 [17], noticing that only those potentials that correspond to the parameter sets that exist inside the stability region display a minimum that indicates stability.

In order to validate our analytical results we have performed a random Monte-Carlo process selecting a set of points in the parameter space (b, Λ) for which there exist stable, spherical shell solutions, as seen in Fig. 3 [17]. We have obtained these points by fixing $m_- = 1, m_+ \equiv m_+/m_- = 1.5$, and repeating a process of considering random values of $(R = R_i, \sigma_i)$ within the limits set by the stability constrain (20) such that $\sigma_i > \sigma_{0min}(R_i)$ (see eq. (21)). For each point in the set of $(R = R_i, \sigma_i)$ values we derive the stability metric parameters (b, Λ) .

3.2. Stiff matter and pressurless dust fluid shells

Regarding the stiff matter shell the equation of state takes the form

$$p = \sigma. \quad (25)$$

with a surface density of,

$$\sigma(R) = \sigma_0 R^{-4} \quad (26)$$

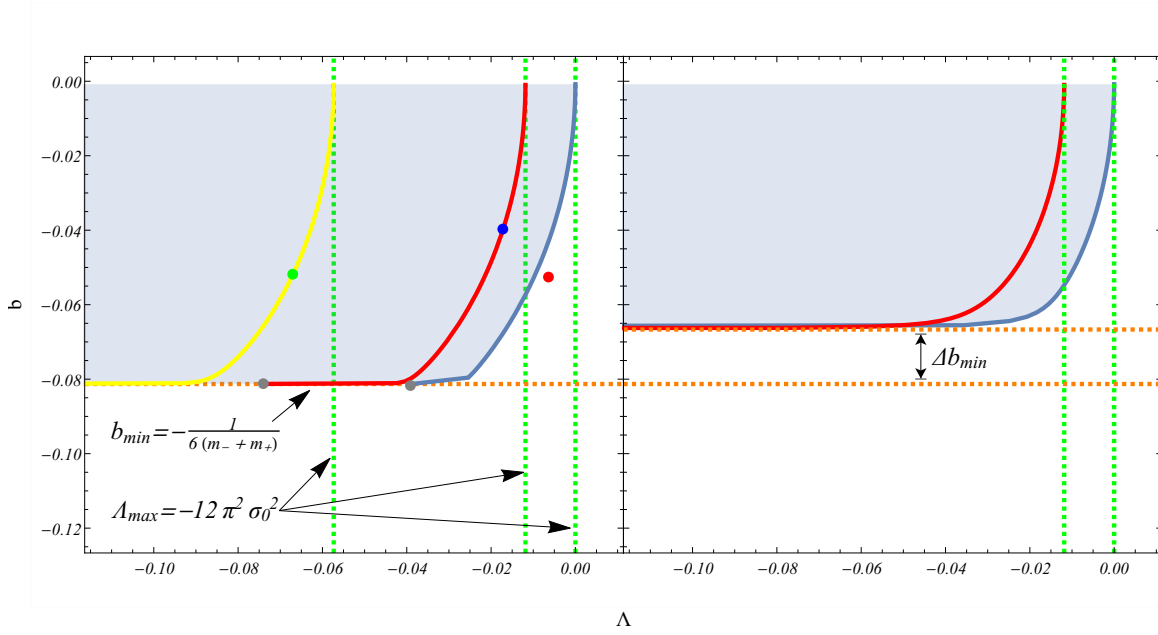


Figure 1. We see the how the stability regions (light blue region) vary for two cases of exterior masses of the shell. Each of the different colored curves correspond to different values of the surface density $\sigma_0 \equiv \sigma_{0min} + \Delta\sigma > \sigma_{0min}$. The left panel corresponds to $m_+ = 1.05$ and the right to $m_+ = 1.5$.

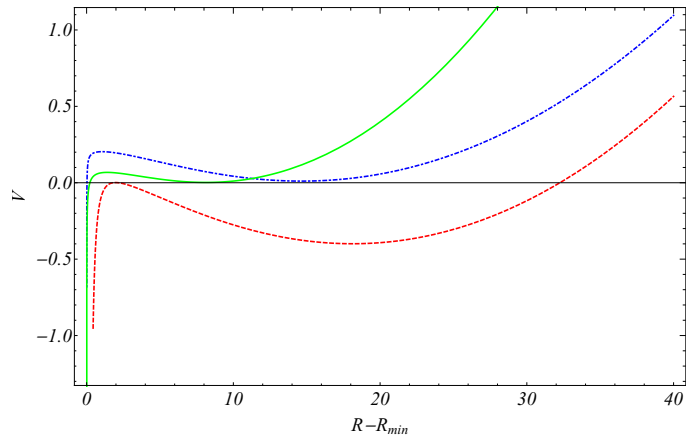


Figure 2. The potential (15) for the values of (b, Λ) that correspond to the points highlighted in Fig. 1. We see that the red point of Fig. 1 does not correspond to a stable shell solution.

whereas for the case of the dust fluid shell the equation of state is

$$p = 0. \tag{27}$$

with a surface density,

$$\sigma(R) = \sigma_0 R^{-2} \tag{28}$$

The potentials (12) are,

$$V(R) = 1 - \frac{\Lambda R^2}{3} + 2bR - \frac{(m_- - m_+)^2 R^4}{16\pi^2 \sigma_0^2} - \frac{m_- + m_+}{R} - \frac{4\pi^2 \sigma_0^2}{R^6} \tag{29}$$

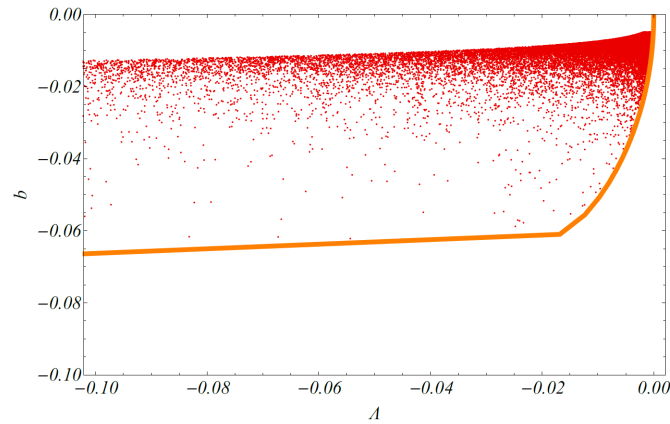


Figure 3. A random Monte-Carlo selection of points that satisfy the shell existence and stability conditions (18 - 21) for $m_+ = 1.5$. The orange line represents the limit of the region which is clearly respected by all the randomly selected points which span the stability region.

and

$$V(R) = 1 - \frac{\Lambda R^2}{3} + 2bR - \frac{(m_- - m_+)^2}{16\pi^2\sigma_0^2} - \frac{m_- + m_+}{R} - \frac{4\pi^2\sigma_0^2}{R^2} \quad (30)$$

for each case respectively. Solving the system (11) for these potentials produces Λ and b of the form,

$$\Lambda(R, \sigma_0) = -\frac{9(m_- - m_+)^2 R^2}{16\pi^2\sigma_0^2} + \frac{6(m_+ + m_-) - 3R}{R^3} + \frac{84\pi^2\sigma_0^2}{R^8}, \quad (31)$$

$$b(R, \sigma_0) = -\frac{(m_- - m_+)^2 R^3}{16\pi^2\sigma_0^2} + \frac{3(m_- + m_+) - 2R}{2R^2} + \frac{16\pi^2\sigma_0^2}{R^7}. \quad (32)$$

for the stiff matter case, and

$$\Lambda(R, \sigma_0) = \frac{3(m_- - m_+)^2}{16\pi^2 R^2 \sigma_0^2} + \frac{6(m_- + m_+) - 3R}{R^3} + \frac{36\pi^2\sigma_0^2}{R^4}, \quad (33)$$

$$b(R, \sigma_0) = \frac{(m_- - m_+)^2}{16\pi^2 R \sigma_0^2} + \frac{3(m_- + m_+) - 2R}{2R^2} + \frac{8\pi^2\sigma_0^2}{R^3}. \quad (34)$$

for the dust fluid shell.

We expect that the range of the metric parameters that allow for stability of the stiff matter shell solutions will be narrower than that of vacuum shell. This is because the potential of eq. (29) contains an extra repulsive term proportional to R^4 , and therefore has the side-effect of diminishing the attraction produced by the anti-deSitter term $\sim \Lambda R^2$ ($\Lambda < 0$) which is very important for the stability of the shell.

The potential (30) that corresponds to the dust fluid shell does not contain any high order terms of R , e.g. R^4 , this benefits the stability at larger R by not constraining the effect of the anti-deSitter term $\sim \Lambda R^2$ ($\Lambda < 0$). This means that the stability range for the case of the dust fluid shell is much wider than the case of the stiff matter equation of state.

4. Conclusion

We have constructed thin, spherical, fluid shell structures in the SRAdS metric and we have proved their stability. These shells are very similar with the gravastar structures [2,3,19–21], if only for the fact that instead of having an interior described by a de sitter metric they are described by the SRAdS metric throughout.

Our analysis could present the opportunity for interesting extensions, including the investigation of the existence and stability of spherical fluid shells in the context of various metrics. Perhaps one could consider a non continuous metric broken up in two pieces, half containing a Schwarzschild term and half containing a Rindler term.

Arguably, the most important extension of our study would be the investigation of the observational effects produced by these types of shell structures. We can study the lensing patterns produced by the lightlike geodesics along the lines of Refs [22,23]. Such observational signatures can directly compared with those of gravastars [24]. Lastly, it would be interesting to investigate non-spherical fluid shells in the context of rotating spacetimes coupled with the cosmological constant.

Funding: This research is co-financed by Greece and the European Union (European Social Fund - ESF) through the Operational Programme "Human Resources Development, Education and Lifelong Learning 2014-2020" in the context of the project "Scalar fields in Curved Spacetimes: Soliton Solutions, Observational Results and Gravitational Waves" (MIS 5047648).

References

1. Israel, W. Singular hypersurfaces and thin shells in general relativity. *Nuovo Cim. B* **1966**, *44S10*, 1. [Erratum: *Nuovo Cim. B* **48**, 463 (1967)], doi:10.1007/BF02710419.
2. Mazur, P.O.; Mottola, E. Gravitational vacuum condensate stars. *Proc. Nat. Acad. Sci.* **2004**, *101*, 9545–9550, [gr-qc/0407075]. doi:10.1073/pnas.0402717101.
3. Visser, M.; Wiltshire, D.L. Stable gravastars: An Alternative to black holes? *Class. Quant. Grav.* **2004**, *21*, 1135–1152, [gr-qc/0310107]. doi:10.1088/0264-9381/21/4/027.
4. Lobo, F.S. Stable dark energy stars. *Class. Quant. Grav.* **2006**, *23*, 1525–1541, [gr-qc/0508115]. doi:10.1088/0264-9381/23/5/006.
5. DeBenedictis, A.; Horvat, D.; Ilijic, S.; Kloster, S.; Viswanathan, K. Gravastar solutions with continuous pressures and equation of state. *Class. Quant. Grav.* **2006**, *23*, 2303–2316, [gr-qc/0511097]. doi:10.1088/0264-9381/23/7/007.
6. Ansoldi, S. Spherical black holes with regular center: A Review of existing models including a recent realization with Gaussian sources. Conference on Black Holes and Naked Singularities, 2008, [arXiv:gr-qc/0802.0330].
7. Alestas, G.; Perivolaropoulos, L. Evading Derrick's theorem in curved space: Static metastable spherical domain wall. *Phys. Rev. D* **2019**, *99*, 064026, [arXiv:gr-qc/1901.06659]. doi:10.1103/PhysRevD.99.064026.
8. Perivolaropoulos, L. Gravitational Interactions of Finite Thickness Global Topological Defects with Black Holes. *Phys. Rev.* **2018**, *D97*, 124035, [arXiv:gr-qc/1804.08098]. doi:10.1103/PhysRevD.97.124035.
9. Grumiller, D. Model for gravity at large distances. *Phys. Rev. Lett.* **2010**, *105*, 211303, [arXiv:astro-ph.CO/1011.3625]. [Erratum: *Phys. Rev. Lett.* **106**, 039901 (2011)], doi:10.1103/PhysRevLett.106.039901, 10.1103/PhysRevLett.105.211303.
10. Carloni, S.; Grumiller, D.; Preis, F. Solar system constraints on Rindler acceleration. *Phys. Rev. D* **2011**, *83*, 124024, [arXiv:astro-ph.EP/1103.0274]. doi:10.1103/PhysRevD.83.124024.
11. Iorio, L. Solar system constraints on a Rindler-type extra-acceleration from modified gravity at large distances. *JCAP* **2011**, *05*, 019, [arXiv:gr-qc/1012.0226]. doi:10.1088/1475-7516/2011/05/019.
12. Mannheim, P.D.; Kazanas, D. Exact Vacuum Solution to Conformal Weyl Gravity and Galactic Rotation Curves. *Astrophys. J.* **1989**, *342*, 635–638. doi:10.1086/167623.
13. Grumiller, D.; Preis, F. Rindler force at large distances. *Int. J. Mod. Phys. D* **2011**, *20*, 2761–2766, [arXiv:astro-ph.CO/1107.2373]. doi:10.1142/S0218271811020585.
14. Iorio, L. Impact of a Pioneer/Rindler-type acceleration on the Oort cloud. *Mon. Not. Roy. Astron. Soc.* **2012**, *419*, 2226–2232, [arXiv:gr-qc/1108.0409]. doi:10.1111/j.1365-2966.2011.19874.x.
15. Anderson, J.D.; Laing, P.A.; Lau, E.L.; Liu, A.S.; Nieto, M.M.; Turyshev, S.G. Indication, from Pioneer 10 / 11, Galileo, and Ulysses data, of an apparent anomalous, weak, long range acceleration. *Phys. Rev. Lett.* **1998**, *81*, 2858–2861, [gr-qc/9808081]. doi:10.1103/PhysRevLett.81.2858.
16. Lammerzahl, C.; Preuss, O.; Dittus, H. Is the physics within the Solar system really understood? *Astrophys. Space Sci. Libr.* **2008**, *349*, 75–101, [gr-qc/0604052]. doi:10.1007/978-3-540-34377-6_3.
17. Alestas, G.; Kraniotis, G.; Perivolaropoulos, L. Existence and stability of static spherical fluid shells in a Schwarzschild-Rindler-anti-de Sitter metric. *Phys. Rev. D* **2020**, *102*, 104015, [arXiv:gr-qc/2005.11702]. doi:10.1103/PhysRevD.102.104015.
18. Frauendiener, J.; Hoenselaers, C.; Konrad, W. A shell around a black hole. *Classical and Quantum Gravity* **1990**, *7*, 585–587. doi:10.1088/0264-9381/7/4/011.
19. Martin Moruno, P.; Montelongo Garcia, N.; Lobo, F.S.; Visser, M. Generic thin-shell gravastars. *JCAP* **2012**, *03*, 034, [arXiv:gr-qc/1112.5253]. doi:10.1088/1475-7516/2012/03/034.
20. Uchikata, N.; Yoshida, S. Slowly rotating thin shell gravastars. *Class. Quant. Grav.* **2016**, *33*, 025005, [arXiv:gr-qc/1506.06485]. doi:10.1088/0264-9381/33/2/025005.
21. Broderick, A.E.; Narayan, R. Where are all the gravastars? Limits upon the gravastar model from accreting black holes. *Class. Quant. Grav.* **2007**, *24*, 659–666, [gr-qc/0701154]. doi:10.1088/0264-9381/24/3/009.

-
22. Lim, Y.K.; Wang, Q.h. Exact gravitational lensing in conformal gravity and Schwarzschild–de Sitter spacetime. *Phys. Rev. D* **2017**, *95*, 024004, [[arXiv:gr-qc/1609.07633](#)]. doi:10.1103/PhysRevD.95.024004.
 23. Cutajar, D.; Adami, K.Z. Strong lensing as a test for Conformal Weyl Gravity. *Mon. Not. Roy. Astron. Soc.* **2014**, *441*, 1291–1296, [[arXiv:gr-qc/1403.7930](#)]. doi:10.1093/mnras/stu617.
 24. Sakai, N.; Saida, H.; Tamaki, T. Gravastar Shadows. *Phys. Rev.* **2014**, *D90*, 104013, [[arXiv:gr-qc/1408.6929](#)]. doi:10.1103/PhysRevD.90.104013